



Cite this: *Org. Biomol. Chem.*, 2017, **15**, 8535

# Pseudouridine modifications influence binding of aminoglycosides to helix 69 of bacterial ribosomes†

Yogo Sakakibara‡ and Christine S. Chow  \*

Development of antibiotics that target new regions of functionality is a possible way to overcome antibiotic resistance. In this study, the interactions of aminoglycoside antibiotics with helix 69 of the *E. coli* 23S rRNA in the context of complete 70S ribosomes or the isolated 50S subunit were investigated by using chemical probing and footprinting analysis. Helix 69 is a dynamic RNA motif that plays major roles in bacterial ribosome activity. Neomycin, paromomycin, and gentamicin interact with the stem region of helix 69 in complete 70S ribosomes, but have diminished binding to the isolated 50S subunit. Pseudouridine modifications in helix 69 were shown to impact the aminoglycoside interactions. These results suggest a requirement for a specific conformational state of helix 69 for efficient aminoglycoside binding, and imply that this motif may be a suitable target for mechanism-based therapeutics.

Received 28th August 2017,  
Accepted 25th September 2017

DOI: 10.1039/c7ob02147j

rsc.li/obc

## Introduction

The aminoglycoside class of antibiotics is clinically important. The existence of antibiotic-resistant bacteria is a global problem that prompted us to examine the detailed mechanism of action of aminoglycosides, for which questions still remain. Aminoglycosides, as well as several other classes of antibiotics, inhibit bacterial ribosome function by binding to ribosomal RNA (rRNA). Their interactions with specific rRNA motifs disrupt ribosomal proofreading,<sup>1</sup> inhibit tRNA/mRNA translocation,<sup>2</sup> and impact ribosome recycling.<sup>3</sup> Aminoglycosides are composed of a highly conserved 2-deoxystreptamine (2-DOS) core typically connected to an aminosugar (Fig. 1A). Because of the ability to bind RNA, 2-DOS serves as a promising motif for the design of semi-synthetic and modified aminoglycosides with improved activity.<sup>4–11</sup> Elucidating the details of drug binding at the ribosome level is important in order to gain a deeper understanding of target selectivity, particularly because of the highly cationic nature of aminoglycosides and their ability to bind multiple targets.

The primary binding site of the aminoglycosides has been shown to be helix 44 (h44) of the 30S subunit of bacterial ribosomes,<sup>12–15</sup> which also involves intersubunit bridge B2a region and helix 69 (H69) of the 50S subunit.<sup>16</sup> Bridge B2a

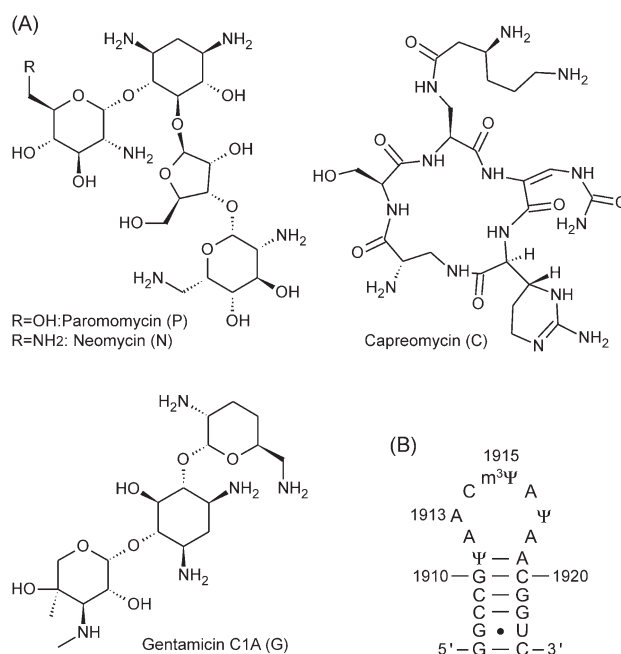


**Fig. 1** (A) Chemical structures of aminoglycoside and peptide antibiotics, paromomycin (P), neomycin (N), gentamicin C1A (G), and capreomycin (C), are shown. (B) The secondary structure of H69 is given (Ψ, pseudouridine; m<sup>3</sup>Ψ, 3-methylpseudouridine).

Department of Chemistry, Wayne State University, Detroit, MI 48202, USA.

E-mail: cchow@wayne.edu

† Electronic supplementary information (ESI) available: Fig. S1–S3. See DOI: 10.1039/c7ob02147j

‡ Current address: KAN Research Institute, Inc., Kobe, Hyogo 650-0047, Japan.

comprises part of the aminoacyl-tRNA site (A site), which plays an important role in tRNA selection by monitoring codon–anticodon interactions.<sup>14,15</sup> Previous studies revealed that aminoglycosides interact with h44 and induce an extrahelical

nucleotide conformation of A1492 and A1493.<sup>14,15,17,18</sup> Similar base orientations were observed in structures of ribosomes complexed with cognate tRNA and mRNA,<sup>14,15</sup> suggesting that aminoglycosides stabilize the h44-mRNA-tRNA complex and cause decoding errors.

A combined X-ray crystallography and single-molecule imaging approach revealed that neomycin also interacts directly with H69 and induces global structural changes in the ribosome, offering a secondary mechanism for how aminoglycosides inhibit ribosome function.<sup>19</sup> Helix 69 also makes direct contacts with cyclic peptide antibiotics (e.g., viomycin and capreomycin) of the tuberactinomycin family.<sup>20</sup> These studies demonstrated the importance of direct interactions between H69 and antibiotics in perturbing ribosome activity; however, details of the molecular mechanism were still missing, such as the role of conserved modified nucleotides at the subunit interface region.

Helix 69 (Fig. 1B) plays important roles in ribosome function, including subunit association,<sup>21,22</sup> translational fidelity,<sup>23–25</sup> tRNA translocation,<sup>26</sup> translation termination,<sup>21,27–29</sup> and ribosome recycling.<sup>30,31</sup> The B2a interaction between the two subunits is maintained during ribosome translocation, suggesting that the conformation of H69 is flexible and dynamic in order to adapt to structural reorganizations between the ribosomal subunits.<sup>32,33</sup> Previous chemical probing results revealed the importance of conserved pseudouridines in the loop region of H69 in mediating H69 conformations.<sup>34,35</sup> Thus, H69 could be an ideal candidate for drug targeting. In this study, the interactions of aminoglycoside antibiotics were investigated in order to further elucidate the relationship between binding activity and H69 conformational states that may be regulated by modified nucleotides.

## Results and discussion

### Footprinting of aminoglycoside binding to the H69 stem region of 70S ribosomes

Crystal structures of *E. coli* 70S ribosomes with aminoglycoside and peptide antibiotics revealed their interactions with H69;<sup>3,20</sup> however, the relationship between binding, H69 solution structure, and post-transcriptional modifications was less clear. To probe the binding of aminoglycoside and peptide antibiotics, dimethylsulfate (DMS) footprinting analysis with sodium borohydride and aniline treatment was performed in the presence of the drugs.<sup>13</sup> Methylation by DMS at the N7 of G followed by reduction is known to cause instability of the glycosidic linkage in the presence of a base such as aniline.<sup>36</sup> Products of the DMS/borohydride/aniline reaction with 23S rRNA in context of 70S ribosomes (*E. coli*) were analyzed by reverse transcription with a suitable DNA primer in the H69 region. Notable protection of the N7 of G at one specific position, G1922, was observed (Fig. 2A) after aniline treatment when comparing RNA with no drug (lane ND) or incubated with aminoglycosides (lanes N, P, and G). At 5  $\mu$ M drug concentrations, structurally similar aminoglycosides neomycin, paromomycin, and gentamicin protected the N7 of G1922

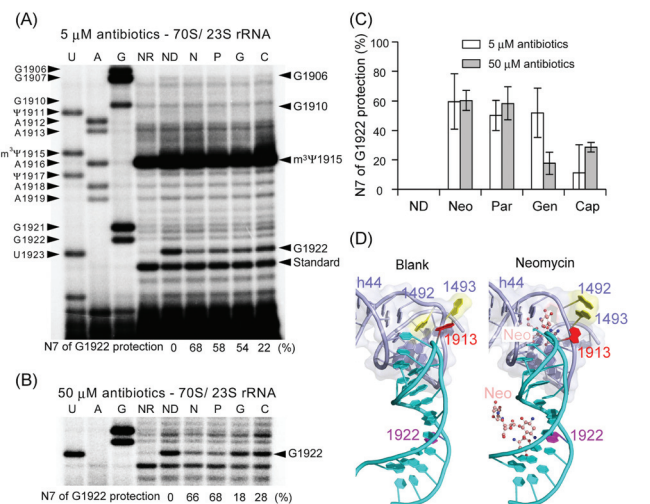


**Fig. 2** Autoradiogram for DMS footprinting followed by primer extension analyses of antibiotic binding to H69 in 70S ribosomes. (A) Data with 5  $\mu$ M antibiotics are shown (U, A, and G sequencing; NR, no DMS; ND, no drug; N, neomycin; P, paromomycin; G, gentamicin; C, capreomycin). Reverse transcription stops before the DMS modification site, so the product mobility differs from the sequencing lane by one nucleotide. Band intensities were normalized to a non-specific stop site (standard) and % protection of G1922 was calculated relative to ND. (B) Footprinting data in the presence of 50  $\mu$ M antibiotics and (C) summary of % protection (average of triplicate footprinting analyses) of G1922 at 5 and 50  $\mu$ M are given. (D) The crystal structures of H69 from 70S ribosomes with or without neomycin (PDB ID: 4 V6C and 4 V52)<sup>3,33</sup> are shown with A1913 in red, G1922 in magenta, and A1492 and A1493 from h44 in yellow.

from DMS at varying levels, 68, 58, and 54%, respectively. In contrast, weaker protection by the peptide antibiotic capreomycin was observed, even at 50  $\mu$ M drug concentrations (28% at 50  $\mu$ M) (Fig. 2B and C). When the drug concentrations were increased to 50  $\mu$ M, neomycin and paromomycin protected the N7 of G1922 to a similar extent (66 to 68%). In contrast, protection by gentamicin decreased to 18% at the higher drug concentration (Fig. 2B and C).

Gentamicin has a 4,6-substituted 2-DOS moiety instead of the 4,5-substituted 2-DOS found in neomycin and paromomycin (Fig. 1A), which impacts the binding to H69. In a titration experiment, the protection level increased between 5 and 10  $\mu$ M gentamicin, but decreased when the concentration was above 25  $\mu$ M (Fig. S1†). At the higher concentrations, gentamicin appears to have a secondary binding site on H69 or an altered binding mode that leads to different interactions and increased exposure of G1922 (and thus higher DMS reactivity). Similar differences were obtained previously with A-site RNA constructs, in which the 4,6-linked aminoglycoside displayed binding stoichiometries greater than 1 : 1.<sup>11</sup>

In addition to protection of residue G1922, protection at the N7 of G1906 by aminoglycoside antibiotics was also observed, but the product bands had very low intensities likely due to the strong reverse transcription stop at the preceding methylated residue m<sup>3</sup> $\Psi$ 1915 (Fig. 2A). Protection of G1906

and G1922 at the N7 positions suggests that the aminoglycosides bind in the major groove of the H69 stem, as was observed in crystal structures of 70S ribosomes and indicated in NMR studies with H69 RNA constructs (Fig. 2D).<sup>19,37</sup> Footprinting analysis on 70S ribosomes revealed that the binding mode for peptide antibiotic capreomycin to H69 is different from that of the aminoglycosides. Capreomycin was shown to interact with rRNA at the interface of bridge B2a in a crystal structure of 70S ribosomes.<sup>20</sup> The lack of protection in the H69 stem by chemical footprinting is in good agreement with that structure; however, we cannot exclude the possibility that capreomycin-ribosome interactions require the presence of mRNA and tRNAs.

In addition to interactions of aminoglycosides with H69, the known binding site on 16S rRNA (the A site of h44) was also examined by primer extension analysis using the same rRNA samples (from 70S ribosomes) used for H69 footprinting. Neomycin, paromomycin, and gentamicin are known to protect a specific nucleotide, A1408 at N1, in the A site of the 30S subunit from DMS. The N1 methylation can be detected as a direct reverse transcription stop site without sodium borohydride or aniline-induced strand scission.<sup>13</sup> Complete protection of the N1 of A1408 of 16S rRNA in the presence of all three aminoglycosides (5  $\mu$ M) was observed (Fig. S2†). Together, these results indicate that aminoglycosides interact with both h44 and H69 under solution conditions, as observed previously in X-ray crystal structures.<sup>3</sup> In contrast, capreomycin did not protect A1408 of h44 from DMS reactivity. In a crystal structure of 70S ribosomes complexed with capreomycin, it appears that the peptide antibiotic contacts h44 from the opposite side as the aminoglycoside.<sup>20</sup> Therefore, lack of protection from DMS reactivity at residue A1408 by capreomycin is consistent with this altered binding mode.

### H69 as a secondary binding site

To compare relative binding affinities of neomycin for H69 (50S subunit) with the A site (30S subunit), neomycin titrations were performed on 70S ribosomes with DMS reactions (reduction and direct strand scission with aniline in the case of H69) and reverse transcription analysis. Neomycin strongly protected A1408 of h44 (68% relative to the control without neomycin) at 0.5  $\mu$ M (Fig. 3A), whereas at least 10  $\mu$ M of the drug was required for a similar level of protection on H69 (Fig. 3B). The level of protection observed therefore gives approximate dissociation constants ( $K_d$  values) of 0.5  $\mu$ M for h44 and 10  $\mu$ M for H69. Within the context of 70S ribosomes in solution, the greater than 10-fold stronger affinity of neomycin for h44 relative to H69 is in good agreement with apparent  $K_d$  values obtained through biophysical experiments on model A-site RNAs, which range from 60 nM to 1  $\mu$ M, depending on the method and solution conditions employed.<sup>11,17,38,39</sup> Our experimental  $K_d$  value determined by isothermal calorimetry (ITC) under near physiological conditions (20 mM HEPES, 70 mM  $\text{NH}_4\text{Cl}$ , 30 mM KCl, pH 7.3 at 25  $^\circ\text{C}$ ) on a short hairpin A-site RNA was 0.4  $\mu$ M (data not shown). In contrast, the apparent  $K_d$  value of neomycin for a small hairpin H69 RNA with

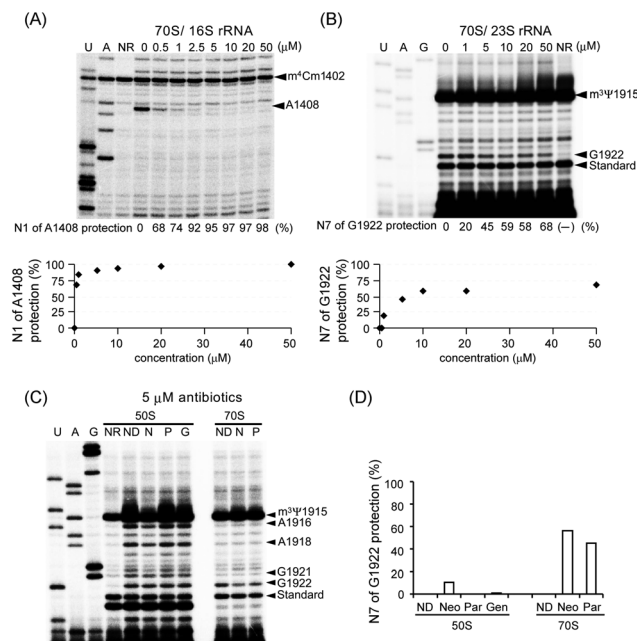


**Fig. 3** Autoradiogram for footprinting analysis of (A) h44 and (B) H69 with increasing (0–50  $\mu$ M) neomycin concentrations (U, A, and G sequencing; NR, no DMS). The same 70S ribosome samples were used for analysis of H69 and h44 to directly compare neomycin binding levels. (C) Footprinting comparison of 50S subunits and 70S ribosomes with 5  $\mu$ M drug concentrations (NR, no DMS; ND, no drug; N, neomycin; P, paromomycin; G, gentamicin). Samples were treated with sodium borohydride followed by aniline-induced strand scission. (D) Summary of % protection of G1922 relative to the standard is given (done in duplicate).

modified bases ( $\Psi$ 1911– $\text{m}^3\Psi$ 1915– $\Psi$ 1917) was 1.1  $\mu$ M under identical conditions, consistent with previous results.<sup>37,40</sup> Combined with the footprinting analysis, H69 appears to be a secondary binding site for aminoglycoside antibiotics, with a three- to 10-fold difference in affinity between the 30S and 50S sites of the complete ribosome. These results illustrate the general lack of selectivity of aminoglycosides, even at the ribosome level.

### Diminished aminoglycoside binding to H69 in isolated 50S subunits

The H69 loop is known to undergo structural rearrangements upon subunit association, which was observed through chemical probing under solution conditions.<sup>35</sup> In contrast, high-resolution X-ray structures of 50S subunits and 70S ribosomes, as well as NMR studies on smaller RNA constructs, all showed similar conformations for the H69 stem portion.<sup>16,41,42</sup> Therefore, the binding mode of aminoglycoside antibiotics to isolated 50S subunits was compared to that of 70S ribosomes, even though binding occurs in the H69 stem region. Weak binding by neomycin to H69 in 50S subunits compared to 70S ribosomes was observed with G1922 protection only at high drug concentrations (50  $\mu$ M) (data not shown). At 5  $\mu$ M concentrations of aminoglycosides, G1922 protection on 70S ribosomes



somes was greater than five-fold higher than protection on 50S subunits (Fig. 3C and D).

Comparison of the probing data on complete 70S ribosomes and isolated 50S subunits (Fig. 3C) revealed another noticeable difference between them – the N7 of G1921 was much more accessible (exposed) towards DMS in the isolated 50S subunits than in 70S ribosomes. Subunit association and intersubunit B2a formation between H69 of the 50S subunit and h44 of the 30S subunit led to protection of A1912, A1916, and A1918 in the H69 loop region from DMS reaction at the N1 position.<sup>35</sup> In contrast, high-resolution X-ray crystal structures did not reveal involvement of either G1921 or G1922 in this interaction.<sup>32</sup> Therefore, the different accessibility of the N7 of G1921 can be interpreted as a local conformational rearrangement in the H69 stem region that is coupled with ribosomal subunit association. Since previous chemical probing studies were consistent with conformational changes in the H69 loop upon subunit association,<sup>35</sup> this result suggests crosstalk between the H69 stem and loop regions on the ribosome level, which was previously observed in H69 model systems.<sup>41,43</sup> Such conformational rearrangements appear to affect the binding scaffold for aminoglycosides within the stem region of H69, as shown by the differences in DMS reactivity at G1922 (*i.e.*, protection by neomycin or paromomycin) between isolated subunits and complete ribosomes.

#### Binding of neomycin alters DEPC reactivity patterns on H69

To further investigate the relationship between antibiotic binding and H69 conformation, diethylpyrocarbonate (DEPC) probing was performed in the presence of aminoglycosides and the cyclic peptide antibiotic. The level of alkylation by DEPC at the N7 position depends on the adenosine environment within a given RNA tertiary structure.<sup>44</sup> Since the readout for this reaction differs from that of the DMS reaction, complementary information can be obtained from this analysis. As shown in Fig. 4A, DEPC reactivity was enhanced three-fold at position 1913 with increasing  $Mg^{2+}$  from 6 to 20 mM, suggesting a more exposed conformation at the higher divalent metal concentration. The opposite effect was observed with added neomycin (5  $\mu$ M). The level of DEPC reactivity at A1913 in the presence of 5  $\mu$ M neomycin was diminished by ~30% compared to the control reaction with no drug (Fig. 4A). In contrast, the other compounds did not cause a decrease in A1913 reactivity, suggesting that they have different binding modes than neomycin. The overall DEPC reactivity did not change in the presence of neomycin as indicated by the similar reactivity pattern in the H68 region (*e.g.*, positions A1847 and A1848, Fig. 4A). These results suggest that neomycin induces a conformational change of the H69 loop, which alters DEPC reactivity. A similar change was observed at A1918 (Fig. 4B). As reported previously,<sup>35</sup> A1918 is not very accessible towards chemical reagents in 70S ribosomes, such that the overall DEPC reactivity is quite low. Nonetheless, A1918 and A1919 reactivity was even further reduced (~40% and ~60%, respectively) in the presence of 5  $\mu$ M neomycin, with similar

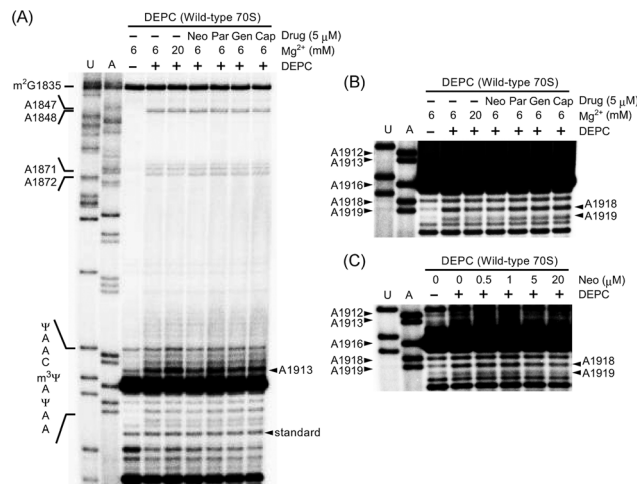


**Fig. 4** (A) Autoradiogram for DEPC probing of 70S ribosomes in the presence of 5  $\mu$ M drug and 20 mM  $Mg^{2+}$ . In the A1871 and A1847 regions, DEPC reactivity is similar in the presence of drugs or high  $Mg^{2+}$  concentrations; therefore, different reactivities of H69 are attributed to different nucleotide conformational states induced by neomycin. (B) An enlarged and higher contrast image of the H69 region is given. Band intensities were normalized to the non-specific band at 1921. (C) Autoradiogram of DEPC footprinting of H69 with increasing concentration of neomycin (0–20  $\mu$ M) is given.

results observed for higher  $Mg^{2+}$  concentrations (Fig. 4B and C). In contrast, only minimal (less than 10%) changes in DEPC reactivity were observed at A1918 and A1919 with paromomycin, gentamicin, or capreomycin.

The different impact of aminoglycoside binding on residue A1913 is consistent with previous results obtained with H69 model constructs. Differing changes in fluorescence were observed upon titration of the aminoglycosides with pseudouridylated H69 containing a 2-aminopurine substitution at position 1913.<sup>40</sup> In that case, neomycin binding had the biggest impact on the H69 loop conformation relative to the other aminoglycosides, and similar increases in fluorescence were observed with  $Mg^{2+}$  titrations. However, for DEPC probing at A1913, opposite trends were observed with  $Mg^{2+}$  and neomycin titrations, suggesting different ligand-induced conformational states. In the presence of neomycin, A1913 could be interacting with another component of the ribosome making it less reactive. In 70S crystal structures containing aminoglycosides,<sup>3</sup> A1913 is projected towards h44 and the N7 position appears to be solvent accessible; however, the DEPC probing data suggest that the N7 is less accessible under the given solution conditions when neomycin is present. A detailed mechanism for the binding and conformational rearrangement induced by neomycin is not known, but the activity is consistent with the observation that only neomycin induces a different H69 loop structure and causes a more open conformation in the smaller model RNA systems.<sup>35,40</sup> Combined with the DMS probing results, it is inferred that the H69 conformational change with concomitant chemical protection is induced by the interaction of neomycin with the H69 stem in 70S ribosomes.

## Pseudouridine modifications play a role in aminoglycoside binding to H69

In nature, RNA is modified at many specific sites in order to provide functional advantages or to expand the genetic code.<sup>45</sup> The H69 loop region contains three pseudouridines ( $\Psi$ ) (Fig. 1B). Previous probing experiments with SHAPE chemistry revealed a disordered H69 conformation in 70S ribosomes isolated from a pseudouridine-deficient strain RluD(-), which is lacking H69 modifications. Therefore,  $\Psi$  modifications in the H69 loop region are associated with modulation of the conformational states.<sup>34,35,46,47</sup> As such, we hypothesized that a lack of  $\Psi$ s in H69 might also affect the binding interactions with aminoglycoside antibiotics. A low level of DMS protection ( $\sim 20\%$ ) at G1922 in RluD(-) 70S ribosomes was observed at 5  $\mu\text{M}$  neomycin and paromomycin, with higher levels ( $\sim 50\%$ ) at 50  $\mu\text{M}$  concentrations (data were normalized to U1915, a non-specific stop site) (Fig. 5A and B). Protection on H69 by gentamicin and capreomycin was not observed in RluD(-) 70S ribosomes at 5  $\mu\text{M}$  drug concentrations. It should be noted that the resolution of these data was lower than that observed with wild-type *E. coli* ribosomes due to higher levels of non-specific degradation of the unmodified rRNA during the process of aniline-induced strand scission, possibly due to a less compact tertiary structure. In comparing the 5  $\mu\text{M}$  neomycin binding data between wild-type and RluD(-) 23S rRNA, the lower level of DMS protection at G1922 on the unmodified RNA suggested an approximate 10-fold reduction in binding affinity in the context of 70S ribosomes.

Aminoglycoside antibiotics demonstrate similar binding affinities to h44 within the context of RluD(-) and wild-type

70S ribosomes, with complete protection at A1408 (direct DMS probing) (Fig. 5C). Thus, loss of  $\Psi$  modifications in H69 in the 50S subunit did not appear to influence aminoglycoside interactions with the A-site of the 30S subunit. Since bridge B2a formation was observed through protection of residues A1912 and A1918 as with wild-type ribosomes, it appears that the conditions used in this experiment were sufficient to favor 70S ribosome formation. Therefore, the possibility of RluD(-) 70S ribosome dissociation leading to the diminished binding of aminoglycosides to H69 was excluded. As with wild-type ribosomes, capreomycin did not show any interaction at A1408 in the RluD(-) 70S ribosomes (Fig. 5C).

DEPC probing of RluD(-) 70S ribosomes revealed no change of the H69 conformation, particularly at A1913, in the presence of antibiotics (Fig. 5D). These results suggested that loss of  $\Psi$  modifications altered the H69 loop conformational states that were induced upon aminoglycoside binding to the stem region of H69. This result is consistent with previous studies employing smaller model RNAs in which binding to unmodified and modified variants of H69 by aminoglycosides was similar in terms of affinity, but only the modified RNA underwent significant conformational changes at A1913 in the presence of neomycin.<sup>40</sup> Another difference between the wild-type and RluD(-) rRNAs occurred at G1910 (Fig. 5A). The N7 of G1910 exhibited strong reactivity towards DMS in RluD(-) 70S ribosomes. This level of reactivity was not observed in wild-type 70S ribosomes or 50S subunits (Fig. 2A and 3C). Even though we cannot exclude the possibility that the strong primer extension stop at m<sup>3</sup> $\Psi$ 1915 masks detection of the G1910 band in wild-type 23S rRNA, our data suggest that a change in the H69 loop conformation caused by loss of  $\Psi$  modification also influences the H69 stem conformation.<sup>35,48</sup>

## Biological implications of neomycin binding to H69

Aminoglycoside antibiotics-H69 interactions within the ribosome have been observed previously in high-resolution X-ray crystal structures,<sup>3</sup> and their influence on ribosome dynamics has been studied at the single molecule level.<sup>19,49</sup> A comparison of X-ray structures of 70S ribosomes at different stages of translation revealed the flexible nature of H69 (Fig. 6) and demonstrated its ability to adopt a variety of conformational states.<sup>3,29,50-56</sup> The binding of aminoglycoside antibiotics appear to further expand the range of conformational states of H69, as shown in Fig. 6. Despite this detailed knowledge about H69, information on its solution conformational changes at the nucleotide level, particularly in the presence of drug molecules, was still lacking. The impact of modified nucleotides on these processes was relatively unexplored. In this work, we provide evidence that aminoglycoside antibiotics interact with the stem region of H69 in 70S ribosomes under solution conditions. In particular, neomycin demonstrated moderate affinity ( $\mu\text{M}$ ) and induced conformational changes of H69 that could be detected with chemical probes that report on nucleotide accessibility. These probing experiments also revealed a role for H69 pseudouridylation in mediating the interactions with aminoglycoside antibiotics.

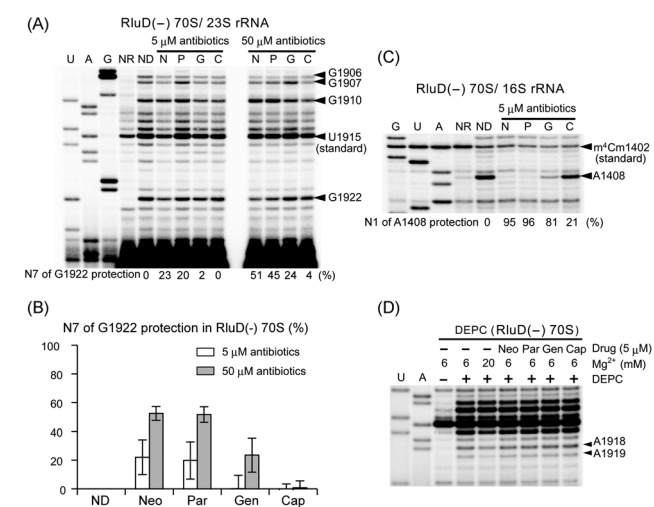


**Fig. 5** (A) Autoradiogram for DMS reactions (sodium borohydride/aniline treatment) on H69 in RluD(-) 70S ribosomes under different drug concentrations. (B) Quantified gel data with % protections at 5 and 50  $\mu\text{M}$  drug concentrations are compared. (C) Autoradiogram for DMS footprinting (no aniline) of h44 in RluD(-) 70S ribosomes (the same ribosome samples as in panel (A)) is shown. (D) Autoradiogram for DEPC footprinting of H69 in RluD(-) 70S ribosomes in the presence of antibiotics is given.

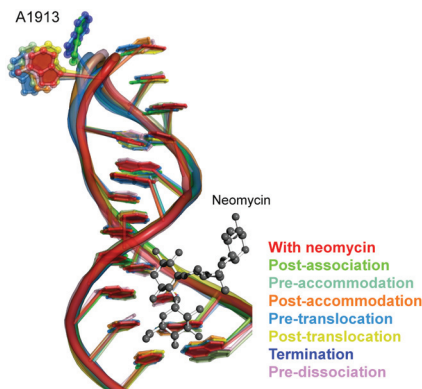


**Fig. 6** The positioning of H69 nucleotides in crystal structures of 70S ribosomes under various conditions or stages of translation is shown (PDB ID: 4 V52 with neomycin;<sup>3</sup> 4 V6A post-association;<sup>50</sup> 4 V5G pre-accommodation;<sup>51</sup> 4 V6F post-accommodation;<sup>52</sup> 4 V9 K pre-translocation;<sup>53</sup> 4 V5F post-translocation;<sup>54</sup> 4 V5E termination;<sup>29</sup> 4 V5A pre-dissociation<sup>55</sup>). Structures for the H69 region were aligned through the stem region. Residue A1913 and neomycin are shown in ball-and-stick representation.

The results presented in this report indicate that neomycin, paromomycin, and gentamicin bind to the H69 stem and protect positions G1922 and G1906 from DMS reactivity, even at low drug concentrations (5  $\mu$ M). This binding mode is in good agreement with X-ray and NMR data.<sup>3,37</sup> The binding of aminoglycosides to H69 is believed to be a secondary interaction relative to the A site (h44) because of the stronger DMS protection pattern at residue A1408 and higher affinity for this 16S rRNA motif as revealed by titration experiments. The possibility of synergistic binding of aminoglycosides to H69 and h44 cannot be excluded, since they are located in close proximity within the 70S ribosome and make contact with one another. Furthermore, only weak binding of aminoglycosides to H69 was observed with isolated 50S subunits. Indeed, synergistic effects of H69 and h44 in drug susceptibility have been proposed for different types of antibiotics. For example, Monshupanee *et al.* noted the importance of methyl modification at both C1409 of h44 and C1920 of H69 in enhancing drug sensitivity to capreomycin.<sup>57</sup> It is not clear, however, whether the enhanced sensitivity is related to direct alterations of drug interactions by methylation or through indirect effects such as methyl-induced conformational changes of H69 and/or h44. Nonetheless, increased sensitivity by a single methylation event on H69 suggested conformational alterations of this dynamic motif. Such effects could be further impacted by the presence of  $\Psi$  modifications. Thus, H69 may play an important role in the activity of aminoglycoside antibiotics together with h44.

Chemical probing with DMS and DEPC showed that neomycin alters the H69 loop conformation upon binding, but paromomycin and gentamicin displayed different effects on nucleotide accessibility, despite their structural similarities to neomycin (Fig. 1A). The biological function of the neomycin-induced H69 conformational change is likely to be important.

Indeed, toe-printing analyses with aminoglycoside antibiotics showed that neomycin has a stronger influence than paromomycin on POST-to-PRE ribosome back translocation.<sup>58</sup> Single-molecule experiments showed that neomycin-bound ribosomes had an increased population of the hybrid-tRNA configuration over the classical-tRNA configuration with increasing concentrations of the drug. Other aminoglycosides did not show such transitions in the ribosome configurations.<sup>59</sup> Single-molecule studies further revealed that neomycin, but not structurally similar kanamycin, altered global ribosome states and stabilized an intermediate state.<sup>19</sup> These results showed that a stabilized intermediate state dominated when greater than 5  $\mu$ M neomycin was present. Consistent with those reports, the chemical probing data at 5  $\mu$ M neomycin showed protection of the H69 stem residue G1922 with concomitant altered accessibility of H69 loop nucleotides. Thus, the DMS and DEPC probing data provide further evidence that neomycin has a secondary binding mode and activity. Furthermore, since the binding modes of aminoglycosides on h44 of the 30S subunit are similar,<sup>3,12</sup> it can be suggested that the H69 conformational state specifically induced by neomycin influences the global ribosome conformation or tRNA positioning as observed in single-molecule studies, thus correlating with their differing biological activities.<sup>58,59</sup>

We also observed lower binding affinity of aminoglycosides for  $\Psi$ -deficient H69 within ribosomes. More specifically, the ability of aminoglycosides to protect specific nucleobases and/or alter the H69 loop conformation was reduced in 70S ribosomes lacking  $\Psi$ s on H69 (from the RluD(–) strain). We also observed increased accessibility of G1910 N7 in  $\Psi$ -deficient ribosomes, suggesting a more open major-groove conformation of the unmodified H69 stem. Previously, we proposed that  $\Psi$  modifications cause H69 to favor a more closed state with lower nucleotide accessibility, and also noted the possible existence of cross-talk between the stem and loop region of H69.<sup>35,48</sup> Conversely, it is suggested that the lack of loop  $\Psi$  residues and structural rearrangements cause indirect alterations of the H69 stem conformation as well, resulting in less favorable interactions with aminoglycosides. Within a more complex biological system, other ribosome components likely play roles in modulating key conformational changes of H69. Therefore, further studies to understand the relationship between rRNA conformation, ligand binding, and post-transcriptional modifications will be necessary in order to fully understand antibiotic mechanisms or drug resistance, as well as to develop novel rRNA-targeting compounds.

## Conclusions

Our findings highlight the role of induced or stabilized H69 conformations by aminoglycoside antibiotics, which may explain observations such as neomycin altering ribosome translational states or tRNA positioning. These results further emphasize the significant functional roles of H69 in the ribosome, and suggest that developing unique antibiotics targeting



H69 of bacterial ribosomes by disturbing its ribosomal states and tRNA-sensing mechanisms could be valuable. Overall, we observed that the H69 stem region undergoes conformational rearrangements coupled with ribosomal subunit association and changes in the loop region, which are affected by both small molecule ligands and pseudouridylation. Although aminoglycosides are known to have a high level of non-specific interactions with nucleic acids, the binding mechanism with H69 features a specific role for pseudouridine and the 6'-amino functionality of neomycin that differs in paromomycin (6'-OH). Importantly, these results suggest that small molecules could be developed that recognize not only a bacterial over eukaryotic RNA such as the functionally important H69, but also a specific modification status of the ribosome.

## Experimental

### Ribosome isolation

Ribosomes were prepared as described elsewhere.<sup>60</sup> Simply, *E. coli* MRE600 or RluD-deficient (RluD(-)) *E. coli* cells were grown to 0.5 OD<sub>600</sub> and cell pellets were collected. Cell pellets were resuspended in lysis buffer (20 mM HEPES, pH 7.4 at 4 °C, 10 mM MgCl<sub>2</sub>, 100 mM NH<sub>4</sub>Cl, 4.6 mM 2-mercaptoethanol, and 0.5 mM EDTA) and lysed by passing twice through a French press at 12 000 psi. Lysate was centrifuged twice for 30 min at 11 000 rpm followed by ultracentrifugation for 4 h at 42 000 rpm. Crude ribosome pellets were gently resuspended in ribosome buffer (20 mM HEPES, pH 7.4 at 4 °C, 1 mM MgCl<sub>2</sub>, 200 mM NH<sub>4</sub>Cl, and 4.6 mM 2-mercaptoethanol for subunit isolation and 20 mM HEPES, pH 7.4 at 4 °C, 6 mM MgCl<sub>2</sub>, 100 mM NH<sub>4</sub>Cl, and 0.6 mM 2-mercaptoethanol for 70S ribosome isolation). The crude ribosome solution was layered on a 10–30% sucrose gradient containing 1 or 6 mM Mg<sup>2+</sup>. Ribosomes were separated by centrifugation at 19 000 rpm for 18 h, followed by elution from the bottom of the tube. The peaks of each ribosomal subunit and 70S ribosomes were observed at 260 nm and fractionated. Magnesium concentration of the pooled sucrose solution was adjusted to 10 mM and ribosomes were pelleted by ultracentrifugation for 24 h at 42 000 rpm for subunits and 24 000 rpm for 70S ribosomes. Purity of the subunits and 70S ribosomes was checked by both sucrose gradient and agarose gel electrophoresis of extracted rRNA (Fig. S3†). Isolated subunits and 70S ribosomes were quickly frozen and stored at –80 °C in stock buffer (20 mM HEPES, pH 7.3, 6 mM MgCl<sub>2</sub>, and 30 mM NH<sub>4</sub>Cl).

### DMS and DEPC footprinting in the presence of aminoglycoside and peptide antibiotics

DEPC (diethylpyrocarbonate) and DMS (dimethylsulfate) probing reactions were carried out using a modified literature procedure.<sup>35,36,44,61</sup> The isolated 70S ribosomes were incubated for reactivation at 37 °C for 15 min under the following conditions; 20 mM HEPES, 6 mM Mg<sup>2+</sup>, 100 mM NH<sub>4</sub>Cl, pH 7.3 at 37 °C. Buffer conditions were adjusted for DMS footprinting (80 mM HEPES, 6 mM Mg<sup>2+</sup>, 100 mM NH<sub>4</sub>Cl, pH 7.3 at 37 °C)

and ribosome concentration was adjusted to 0.3 μM by dilution. The 70S ribosomes were again incubated at 37 °C for 10 min in footprinting buffer. Each antibiotic tested (neomycin, paromomycin, gentamicin, and capreomycin stocks in footprinting buffer at 100 μM or 1 mM) was added at a 5 to 50 μM final concentration, and incubated at 37 °C for an additional 10 min. DMS or DEPC footprinting was initiated by the addition of 2 μL DMS in cold ethanol (20 mM DMS final reaction concentration) or 2 μL DEPC for 40 μL final volume, and incubation proceeded at 37 °C for 10 min. The reaction mixture was quickly terminated by adding 10 μL stop buffer (3 M 2-mercaptoethanol, 1 M Tris-HCl, pH 7.5 at RT, 10 mM MgCl<sub>2</sub>) followed by ethanol precipitation. The pelleted ribosome was dissolved in buffer (50 mM Tris-HCl, 2 mM EDTA, pH 7.5 at RT). The rRNAs were prepared by general phenol-chloroform extraction. All footprinting assays were performed at least three times independently, unless otherwise noted.

### Sodium borohydride and aniline-induced strand scission at N7 of G

Sodium borohydride and aniline-induced strand scission was performed as follows. The chemically probed rRNAs were dissolved in 10 μL of 1 M Tris-HCl (pH 8.3) with 2.5 μg of carrier tRNA, and incubated on ice in the dark for 30 min with 10 μL of freshly prepared 0.2 M sodium borohydride. The reaction was quenched by adding 10 μL of 3 M sodium acetate (pH 5.3) and cold ethanol, and then quickly precipitated by centrifugation. The RNA pellet was rinsed with 70% ethanol and dried briefly. The RNA pellet was dissolved in 10 μL of freshly prepared 1 M aniline-acetate (pH 4.5), and incubated at 60 °C for 20 min. The reaction was terminated by putting the tube on ice for 1 min followed by addition of 100 μL of 0.2 M sodium acetate (pH not adjusted). The quenched solution was extracted with phenol-chloroform, followed by an additional chloroform extraction and ethanol precipitation. The pelleted rRNA was used for reverse transcription as described previously.<sup>34,35</sup>

## Conflicts of interest

There are no conflicts to declare.

## Acknowledgements

We thank G. Garcia and A. Mankin for providing the *E. coli* strains, P. Cunningham for providing access to equipment for ribosome isolations, A. Mohamed for assistance in sample preparation for ITC experiments, and J. Jiang for assistance with figures and helpful discussions. This project was supported by the NIH (GM087596).

## References

- 1 J. Davies, L. Gorini and B. D. Davis, *Mol. Pharmacol.*, 1965, **1**, 93.

- 2 P. Edelmann and J. Gallant, *Cell*, 1977, **10**, 131.
- 3 M. A. Borovinskaya, R. D. Pai, W. Zhang, B. S. Schuwirth, J. M. Holton, G. Hirokawa, H. Kaji, A. Kaji and J. H. Cate, *Nat. Struct. Mol. Biol.*, 2007, **14**, 727.
- 4 T. J. Baker, N. W. Luedtke, Y. Tor and M. Goodman, *J. Org. Chem.*, 2000, **65**, 9054.
- 5 E. C. Böttger, B. Springer, T. Prammananan, Y. Kidan and P. Sander, *EMBO Rep.*, 2001, **2**, 318.
- 6 T. Hermann, *Curr. Opin. Struct. Biol.*, 2005, **15**, 355.
- 7 N. W. Luedtke, P. Carmichael and Y. Tor, *J. Am. Chem. Soc.*, 2003, **125**, 12374.
- 8 T. Matsushita, W. Chen, R. Juskeviciene, Y. Teo, D. Shcherbakov, A. Vasella, E. C. Böttger and D. Crich, *J. Am. Chem. Soc.*, 2015, **137**, 7706.
- 9 A. Pushechnikov, M. M. Lee, J. L. Childs-Disney, K. Sobczak, J. M. French, C. A. Thornton and M. D. Disney, *J. Am. Chem. Soc.*, 2009, **131**, 9767.
- 10 X. Wang, M. T. Migawa, K. A. Sannes-Lowery and E. E. Swayze, *Bioorg. Med. Chem. Lett.*, 2005, **15**, 4919.
- 11 C. H. Wong, M. Hendrix, E. S. Priestley and W. A. Greenberg, *Chem. Biol.*, 1998, **5**, 397.
- 12 A. P. Carter, W. M. Clemons, D. E. Brodersen, R. J. Morgan-Warren, B. T. Wimberly and V. Ramakrishnan, *Nature*, 2000, **407**, 340.
- 13 D. Moazed and H. F. Noller, *Nature*, 1987, **327**, 389.
- 14 J. M. Ogle, D. E. Brodersen, W. M. Clemons Jr., M. J. Tarry, A. P. Carter and V. Ramakrishnan, *Science*, 2001, **292**, 897.
- 15 J. M. Ogle, F. V. Murphy IV, M. J. Tarry and V. Ramakrishnan, *Cell*, 2002, **111**, 721.
- 16 M. M. Yusupov, G. Z. Yusupova, A. Baucom, K. Lieberman, T. N. Earnest, J. H. Cate and H. F. Noller, *Science*, 2001, **292**, 883.
- 17 D. Fourmy, M. I. Recht, S. C. Blanchard and J. D. Puglisi, *Science*, 1996, **274**, 1367.
- 18 Q. Vicens and E. Westhof, *Structure*, 2001, **9**, 647.
- 19 L. Wang, A. Pulk, M. R. Wasserman, M. B. Feldman, R. B. Altman, J. H. Cate and S. C. Blanchard, *Nat. Struct. Mol. Biol.*, 2012, **19**, 957.
- 20 R. E. Stanley, G. Blaha, R. L. Grodzicki, M. D. Strickler and T. A. Steitz, *Nat. Struct. Mol. Biol.*, 2010, **17**, 289.
- 21 I. K. Ali, L. Lancaster, J. Feinberg, S. Joseph and H. F. Noller, *Mol. Cell*, 2006, **23**, 865.
- 22 U. Maiväli and J. Remme, *RNA*, 2004, **10**, 600.
- 23 K. Kipper, C. Hetényi, S. Sild, J. Remme and A. Liiv, *J. Mol. Biol.*, 2009, **385**, 405.
- 24 A. Liiv, D. Karitkina, U. Maiväli and J. Remme, *BMC Mol. Biol.*, 2005, **6**, 18.
- 25 M. O'Connor and A. E. Dahlberg, *J. Mol. Biol.*, 1995, **254**, 838.
- 26 A. Bashan, I. Agmon, R. Zarivach, F. Schlutzenzen, J. Harms, R. Berisio, H. Bartels, F. Franceschi, T. Auerbach, H. A. Hansen, E. Kossoy, M. Kessler and A. Yonath, *Mol. Cell*, 2003, **11**, 91.
- 27 A. Korostelev, J. Zhu, H. Asahara and H. F. Noller, *EMBO J.*, 2010, **29**, 2577.
- 28 M. Laurberg, H. Asahara, A. Korostelev, J. Zhu, S. Trakhanov and H. F. Noller, *Nature*, 2008, **454**, 852.
- 29 A. Weixlbaumer, H. Jin, C. Neubauer, R. M. Voorhees, S. Petry, A. C. Kelley and V. Ramakrishnan, *Science*, 2008, **322**, 953.
- 30 R. K. Agrawal, M. R. Sharma, M. C. Kiel, G. Hirokawa, T. M. Booth, C. M. Spahn, R. A. Grassucci, A. Kaji and J. Frank, *Proc. Natl. Acad. Sci. U. S. A.*, 2004, **101**, 8900.
- 31 D. N. Wilson, F. Schlutzenzen, J. M. Harms, T. Yoshida, T. Ohkubo, R. Albrecht, J. Buerger, Y. Kobayashi and P. Fucini, *EMBO J.*, 2005, **24**, 251.
- 32 B. S. Schuwirth, M. A. Borovinskaya, C. W. Hau, W. Zhang, A. Vila-Sanjurjo, J. M. Holton and J. H. Cate, *Science*, 2005, **310**, 827.
- 33 W. Zhang, J. A. Dunkle and J. H. Cate, *Science*, 2009, **325**, 1014.
- 34 Y. Sakakibara and C. S. Chow, *J. Am. Chem. Soc.*, 2011, **133**, 8396.
- 35 Y. Sakakibara and C. S. Chow, *ACS Chem. Biol.*, 2012, **7**, 871.
- 36 D. A. Peattie, *Proc. Natl. Acad. Sci. U. S. A.*, 1979, **76**, 1760.
- 37 A. E. Scheunemann, W. D. Graham, F. A. Vendeix and P. F. Agris, *Nucleic Acids Res.*, 2010, **38**, 3094.
- 38 B. Llano-Sotelo, E. F. Azucena Jr., L. P. Kotra, S. Mobashery and C. S. Chow, *Chem. Biol.*, 2002, **9**, 455.
- 39 Y. Wang, K. Hamasaki and R. R. Rando, *Biochemistry*, 1997, **36**, 768.
- 40 Y. Sakakibara, S. C. Abeyirigunawardena, A. C. Duc, D. N. Dremann and C. S. Chow, *Angew. Chem., Int. Ed. Engl.*, 2012, **51**, 12095.
- 41 J. Jiang, R. Aduri, C. S. Chow and J. SantaLucia Jr., *Nucleic Acids Res.*, 2014, **42**, 3971.
- 42 P. Nissen, J. Hansen, N. Ban, P. B. Moore and T. A. Steitz, *Science*, 2000, **289**, 920.
- 43 J. Jiang, D. N. Kharel and C. S. Chow, *Biophys. Chem.*, 2015, **200–201**, 48.
- 44 D. A. Peattie and W. Gilbert, *Proc. Natl. Acad. Sci. U. S. A.*, 1980, **77**, 4679.
- 45 J. Jiang, H. Seo and C. S. Chow, *Acc. Chem. Res.*, 2016, **49**, 893.
- 46 S. C. Abeyirigunawardena and C. S. Chow, *RNA*, 2008, **14**, 782.
- 47 J. P. Desaulniers, Y. C. Chang, R. Aduri, S. C. Abeyirigunawardena, J. SantaLucia Jr. and C. S. Chow, *Org. Biomol. Chem.*, 2008, **6**, 3892.
- 48 M. Sumita, J. Jiang, J. SantaLucia Jr. and C. S. Chow, *Biopolymers*, 2012, **97**, 94.
- 49 J. Noeske, M. R. Wasserman, D. S. Terry, R. B. Altman, S. C. Blanchard and J. H. Cate, *Nat. Struct. Mol. Biol.*, 2015, **22**, 336.
- 50 G. Blaha, R. E. Stanley and T. A. Steitz, *Science*, 2009, **325**, 966.
- 51 T. M. Schmeing, R. M. Voorhees, A. C. Kelley, Y. G. Gao, F. V. Murphy IV, J. R. Weir and V. Ramakrishnan, *Science*, 2009, **326**, 688.
- 52 L. B. Jenner, N. Demeshkina, G. Yusupova and M. Yusupov, *Nat. Struct. Mol. Biol.*, 2010, **17**, 555.



- 53 J. Zhou, L. Lancaster, J. P. Donohue and H. F. Noller, *Science*, 2013, **340**, 1236086.
- 54 Y. G. Gao, M. Selmer, C. M. Dunham, A. Weixlbaumer, A. C. Kelley and V. Ramakrishnan, *Science*, 2009, **326**, 694.
- 55 A. Weixlbaumer, S. Petry, C. M. Dunham, M. Selmer, A. C. Kelley and V. Ramakrishnan, *Nat. Struct. Mol. Biol.*, 2007, **14**, 733.
- 56 J. Jiang, Y. Sakakibara and C. S. Chow, *Isr. J. Chem.*, 2013, **53**, 379.
- 57 T. Monshupanee, S. K. Johansen, A. E. Dahlberg and S. Douthwaite, *Mol. Microbiol.*, 2012, **85**, 1194.
- 58 S. Shoji, S. E. Walker and K. Fredrick, *Mol. Cell*, 2006, **24**, 931.
- 59 M. B. Feldman, D. S. Terry, R. B. Altman and S. C. Blanchard, *Nat. Chem. Biol.*, 2010, **6**, 54.
- 60 G. Blaha, U. Stelzl, C. M. Spahn, R. K. Agrawal, J. Frank and K. H. Nierhaus, *Methods Enzymol.*, 2000, **317**, 292.
- 61 D. Moazed and H. F. Noller, *Cell*, 1986, **47**, 985.